STRONG ELECTROLYTE CONTINUUM THEORY SOLUTION FOR EQUILIBRIUM PROFILES, DIFFUSION LIMITATION, AND CONDUCTANCE IN CHARGED ION CHANNELS

DAVID G. LEVITT
Department of Physiology, University of Minnesota, Minneapolis, Minnesota 55455

ABSTRACT The solution for the ion flux through a membrane channel that incorporates the electrolyte nature of the aqueous solution is a difficult theoretical problem that, until now, has not been properly formulated. The difficulty arises from the complicated electrostatic problem presented by a high dielectric aqueous channel piercing a low dielectric lipid membrane. The problem is greatly simplified by assuming that the ratio of the dielectric constant of the water to that of the lipid is infinite. It is shown that this is a good approximation for most channels of biological interest. This assumption allows one to derive simple analytical expressions for the Born image potential and the potential from a fixed charge in the channel, and it leads to a differential equation for the potential from the background electrolyte. This leads to a rigorous solution for the ion flux or the equilibrium potential based on a combination of the Nernst-Planck equation and strong electrolyte theory (i.e., Gouy-Chapman or Debye-Huckel). This approach is illustrated by solving the system of equations for the specific case of a large channel containing fixed negative charges. The following characteristics of this channels are discussed: anion and mono- and divalent cation conductance, saturation of current with increasing concentration, current-voltage relationship, influence of location and valence of fixed charge, and interaction between ions. The qualitative behavior of this channel is similar to that of the acetylcholine receptor channel.

INTRODUCTION

Previous electrostatic solutions for the potential profile in ion channels have by necessity assumed that the aqueous and channel regions could be modeled by a simple pure dielectric nonconducting medium into which the charged ion or fixed charge group of interest is introduced (1–3). This assumption rules out the application of these solutions to situations where the electrolyte nature of the aqueous medium is important. For example, to determine the effect of a fixed charge at the mouth of an ion channel it is necessary to calculate the potential at the mouth that results from the screening by the counter ions in the solution. In lieu of a better theoretical approach to this problem, the Gouy-Chapman theory has been used to estimate this potential (4). However, there is a qualitative difference between an infinite plane of charge (Gouy-Chapman) and a single fixed charge and, clearly, a more accurate solution is needed. Another example where the electrolyte nature of the aqueous medium must be accounted for is in the calculation of whether diffusion in the bulk solution limits the channel conductance. If, for example, the channel is cation selective, there will be a polarization due to a depletion of positive charges at one mouth and an excess at the other, which tends to increase the rate of bulk diffusion up to and away from the channel. There have been two previous approaches to calculating the magnitude of this effect. Lauger (5) carried out detailed calculations based on the assumption that the bulk solution was everywhere electrically neutral. Andersen (6), using a fundamentally different approach, assumed that the bulk solution was at equilibrium and that the membrane-channel region could be approximated by an equivalent one-dimensional capacitor (whose capacitance was an adjustable parameter). A third example, and the one that will be considered in the most detail here, is related to the problem of finding the ion flux through a channel that contains fixed charges. A realistic solution to this problem must allow for the screening of the fixed charge by counter ions.

The basic difficulty in these problems results from the complicated spatial variation of the dielectric constant: a high dielectric constant ($\epsilon \simeq 80$) in the bulk solutions and in the water-filled ion channel, a low dielectric ($\epsilon \simeq 2$) in the membrane and an intermediate value for the channel protein. The electrostatic solution for the pure dielectric case requires quite involved numerical calculations to determine the potential at each point in space. The combination of this solution with an approach that takes account of the electrolyte nature of the dielectric (e.g., Debye-Huckel) presents a formidable problem. However, it will be shown here that the problem is greatly simplified by

BIOPHYS. J. © Biophysical Society · 0007–3495/85/07/19/13 $1.00
Volume 48 July 1985 19–31

introducing the assumption that the ratio of the dielectric constant of the water to that of the lipid is infinite. In the following sections the motivation for this assumption will be given first. Then the validity of the assumption will be evalulated by comparison with some exact solutions. It will be shown that for most ion channels the error introduced by this assumption is small and of a size similar to that introduced by other uncertainties, such as the value assumed for the dielectric constant of water in the channel. Then, the use of this approximation will be illustrated by finding the continuum solution for the flux through a channel that contains a fixed charge. This problem is examined for two reasons: first, it is the most general type of situation in which this approach can be used, with the two examples discussed above (equilibrium potential at the mouth of a channel that has fixed charges and the bulk solution diffusion limited access to a channel) representing special cases of this more general solution. Secondly, a channel large enough for continuum theory to be applicable and with its selectivity determined simply by a fixed charge may provide a useful model for some biological membrane channels, specifically, the acetylcholine receptor channel.

GLOSSARY

e, q	electron charge and arbitrary charge
z, n	valence of ion and fixed charge
ϵ_w, ϵ_L	dielectric constant of water and lipid
X, Y	axial distance from center of channel
a, b	radius of channel at center and of ion
L	half-length of channel
R, R_0	channel radius at arbitrary position and at end
S	constant E field surface area in channel
S_e	area available to center of ion (Eq. 23a)
D_0, D_e	bulk and channel diffusion coefficient (Eq. 23b)
C, C_0	concentration at X and in bulk solution
Ψ, Φ, U, W	total potential; diffuse plus applied potential; Born image charging potential; and fixed charge potential
E	electric field
J, J_+, J_-	flux, cation flux, and anion flux
I, H	integrals (see Eqs. 16d and 20).

Dimensionless Variables

α (see Eq. A6); $\beta = b/R$; $\gamma = e^2/(kT\epsilon_w a)$; $\delta = L/a$; $\phi = \Phi/(q/\epsilon_w a)$; $\Omega = 4\pi a^3 C_o$; $c = C/C_o$; $e = E/(e/\epsilon_w a^2)$; $g = D_e/D_o$; $j = 4\pi J/(D_o a^2)$; $K = \epsilon_w/\epsilon_L$; $\ell = \delta + r_o$; $r = R/a$; $s = S/a^2$; $s_e = S_e/a^2$; $u = U/(e/\epsilon_w a)$; $w = W/(e/\epsilon_w a)$; $x = X/a$.

BASIC APPROXIMATION OF THE METHOD

Fig. 1 shows a schematic diagram of the spatial arrangement of the dielectric constant for an ion channel. In this diagram (and in the rest of this paper) the dielectric of the protein that forms the channel is neglected. The effect of the channel can be approximated by increasing the effective radius of the high dielectric channel region (1). Also, it is assumed that the water in the channel has a dielectric constant equal to that of bulk water. The electrostatic relations that must hold at the boundary between the water

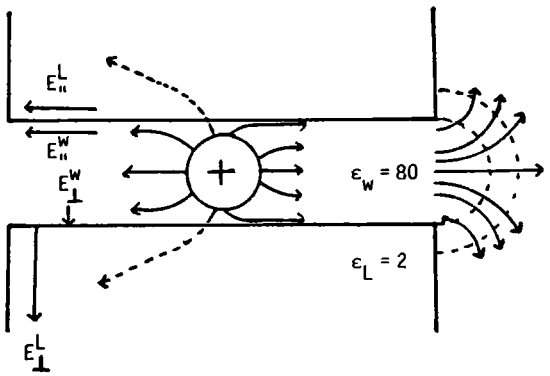

FIGURE 1 Schematic diagram of a water-filled channel through a lipid membrane. The field lines to the right of the ion illustrate the basic assumption that $E^w_\perp$ is zero at the water-lipid interface so that the field lines are constrained to the aqueous region.

and the lipid are

$$E^L_\parallel = E^w_\parallel; \qquad \epsilon_w E^w_\perp = \epsilon_L E^L_\perp, \tag{1}$$

where subscripts $\parallel$ and $\perp$ indicate the E field parallel and perpendicular to the water lipid interface and the superscripts w and L refer to the water and lipid regions, respectively. Also, in the lipid region at the water-lipid interface the parallel and perpendicular components should be of similar magnitudes

$$E^L_\perp \simeq E^L_\parallel. \tag{2}$$

Combining Eqs. 1 and 2

$$E^w_\perp \simeq E^w_\parallel / K \quad K = \epsilon_w/\epsilon_L. \tag{3}$$

Since K (the ratio ϵ_w/ϵ_L) is ~40, the value of $E^w_\perp$ is small compared with that of $E^w_\parallel$. This is the motivation for the following basic approximation: the perpendicular component of E in the aqueous region is zero along the water-lipid interface. This means that the E field lines are confined within the channel and spread into the bulk solution as is illustrated on the right half of Fig. 1.

The above argument is qualitative. To quantitatively evaluate this approximation the Born (image) potential calculated using it will be compared with an exact numerical solution. This calculation provides a simple example of the use of this approximation. The calculation will be made for an ion (charge = q) in the center of a uniform cylindrical pore of radius a and length $2L$ (Fig. 2). The Born potential (Φ_B) is the difference between the potential at the surface of the charged sphere (ion) (radius = b) when it is in the channel (Φ_C) and when it is in a homogeneous dielectric medium (Φ_H). For the homogenous case

$$\Phi_H = \int_b^\infty E_H dx \quad E_H = q/(\epsilon_w X^2). \tag{4}$$

For the pore case the value of E can be obtained using the basic approximation that $E_\perp = 0$ along with a few

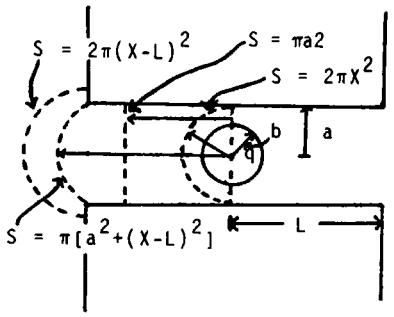

FIGURE 2 Constant E field surface areas (S, dashed lines) that are used to calculate the Born image potential.

additional assumptions. A Gaussian surface (7) is used that has one end in the center of the channel, bisecting the charged sphere, the other end at an arbitrary distance X from the sphere (dashed lines, Fig. 2), and sides coinciding with the pore walls. By symmetry the normal E field is zero at the end in the center of channel and it is zero along the sides due to the basic approximation ($E_\perp = 0$). The surface encloses the charge $q/2$. It will be assumed that E is uniform over the surface at X (with area $S[X]$) so that, by Gauss's law, the value of $E_C(X)$ (E in the channel) is given by

$$\int_S E_C dS = E_C S(X) = 2\pi q/\epsilon_w. \tag{5}$$

This assumption of a constant E surface ($S[X]$) greatly simplifies the problem because it reduces the spatial variation in E (or Φ) to a dependence only on the one-dimensional parameter X, the axial distance from the ion to the surface S.

The area of the constant E surface that will be used here and in the rest of the paper is described by (for a definition of notation, see Glossary)

$$S(X) = \begin{cases} 2\pi X^2 & b < X < a \\ \pi a^2 & a < X < L \\ \pi[a^2 + (X - L)^2] & L < X < L + a \\ 2\pi(X - L)^2 & L + a < X < \infty. \end{cases} \tag{6}$$

The choice of a surface is somewhat arbitrary. This surface (Fig. 2) was chosen both because it provided a reasonable approximation to the exact solution and because of its mathematical simplicity. Somewhat better agreement with the exact solution can be obtained by using surfaces that provide a smoother change in shape near the ion, but the improvement is small and does not justify the increased mathematical complexity.

The Born potential is the difference between Φ_C and Φ_H

$$\Phi_B = \int_b^\infty E_C\, dX - \int_b^\infty E_H\, dX = \int_a^{L+a} E_C\, dX. \tag{7}$$

The results will be expressed in dimensionless variables (small case) with all lengths relative to the pore radius (a) and the electrical field and potential relative to $q/\epsilon_w a^2$ and $q/\epsilon_w a$, respectively. Substituting the expression for $S(X)$ (Eq. 6) into Eq. 5 for E_C and this expression into Eq. 7, the final expression for ϕ_B as a function of channel length ($\delta = L/a$ 1) is

$$\phi_B = 2(\delta - 1 + \pi/4). \tag{8}$$

This relation is plotted in Fig. 3 along with the exact numerical solution of Jordan (8) for two different values of K ($= \epsilon_w/\epsilon_L$).

There are two independent approximations that have gone into this derivation for ϕ_B (Eq. 8). The first is the basic approximation that $E_\perp$ is zero on the pore walls. The second is the assumption of a particular constant E surface. The first approximation is essentially equivalent to assuming that K is infinite. If the ϕ_B for the actual case where $K = 40$ is close to the limiting value when K is infinite, then the ϕ_B for $K = 40$ and $K = 20$ should be nearly equal. As can be seen by comparing the ϕ_B for $K = 20$ and $K = 40$ in Fig. 3, this condition is approximately satisfied for values of the pore half-length to radius ratio ($\delta = L/a$) of $\lesssim 3$. It can also be seen from Fig. 3 that the particular solution for ϕ_B assuming the constant E surface (dashed line) is within 20% of the correct value ($K = 40$) for $\delta < 3$ or $\phi_B \lesssim 4$. For the large membrane channels, which will be considered here, ϕ_B will be in this range so that the error introduced by this approximation is of the same magnitude as other uncertainties, i.e., the value for the dielectric constant of water in the channel or the influence of the channel wall on the effective radius of the high dielectric region of the channel.

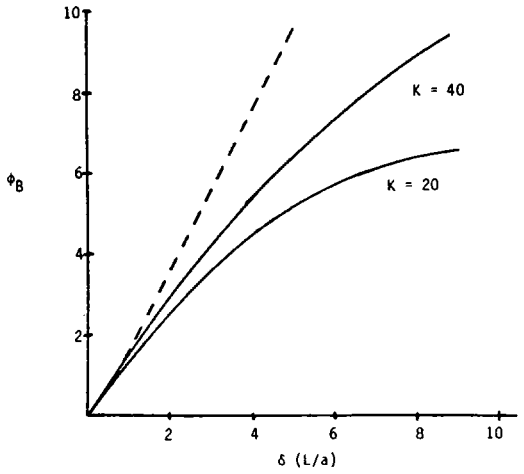

FIGURE 3 Comparison of exact numerical solution (7) for the Born image potential (solid lines) for a K (ϵ_w/ϵ_L) of 20 and 40 with the approximate solution (dashed line, Eq. 8). The dimensionless potential (ϕ_B, in units of $e/\epsilon_w a$) is plotted vs. the dimensionless channel half-length ($\delta = L/a$).

EXACT CONTINUUM SOLUTION FOR THE FLUX THROUGH A CHARGED MEMBRANE CHANNEL

The motivation for solving this problem, in addition to illustrating an application of the basic approximation, is that a large continuum channel with a fixed (negative) charge may provide a useful model for some (cation) selective ion channels, e.g., the acetylcholine receptor channel. In this section the following quantitative features of one specific model will be examined: cation/anion selectivity, divalent/monovalent cation flux and interaction, flux saturation with increasing concentration, dependence of flux on the channel fixed charge and ion radius, and the current-voltage relationship.

It will be assumed that the ion flux of the ith ion (J_i) is described by the Nernst-Planck equation

$$J_i = -D_e^i S_e^i [dC_i/dX + (z_i e/kT) C_i \, d\Psi_i/dX], \qquad (9)$$

where D_e^i and S_e^i are the effective diffusion coefficient and area, and Ψ_i is the generalized potential and includes all the long-range forces on the ion. The generalized potential will be written as a sum of three terms: the Born image charging potential (U), the potential from the fixed charge (W), and the rest (Φ), which is the potential that arises from the applied voltage and all the other ions in the system. The potential Φ is the central function in the solution. It provides the coupling between the ions and other potential functions (U and W) because all the potentials act on each ion and each ion contributes to Φ. This potential (Φ), which will be referred to as the diffuse charge potential, is equivalent to the potential that is used in Debye-Huckel theory and it is through this function that ionic strength effects are incorporated into the solution. The mathematical description of each of these potentials will be described below.

Born Image Charging Potential (U)

As shown above, the Born potential at the surface of a sphere of radius a of charge q can be written in the form: $\Phi_B(q) = (q/\epsilon_w a)\phi_B$, where ϕ_B does not depend on the charge. The potential energy (zeU) required to transfer an ion (charge ze) from the bulk solution to the position x in the channel is equal to the energy required to transfer the charge ze from infinity to the ion

$$zeU = \int_0^{ze} \Phi_B(q)dq = (ze)^2\phi_B/(2\epsilon_w a)$$
$$U = ze\phi_B/(2\epsilon_w a). \qquad (11)$$

An analytical expression for ϕ_B was derived above for the case of an ion in the center of a uniform cylindrical pore. A similar approach can be used to find an expression for an ion at an arbitrary position in a pore of varying cross section (see Appendix).

Fixed Charge Potential (W)

For the case where the fixed charge ($q = ne$) is in the center of a symmetrical channel, its contribution to the E field can be determined using the same Gaussian surface that was used in the derivation of the Born image potential (Fig. 2). The field is, by symmetry, zero for the end of the Gaussian surface in the center of the channel and the field at the other end (position X, surface area $S[X]$) is described by

$$E = 2\pi ne/[\epsilon_w S(X)]. \qquad (12)$$

The fixed charge potential is thus

$$W = -(2\pi ne/\epsilon_w) \int_\infty^X dx/S(x). \qquad (13)$$

The practical requirements of solving the differential equation (see below) necessitate making the assumption that the solution is well-stirred up to a certain distance from the channel mouth and this distance must be used in place of infinity for the lower limit of the integral in Eq. 13. A somewhat more complicated expression is needed if the fixed charge is not at the center of a symmetrical channel (see the section entitled Analytical Expressions for Born Image and Fixed Charge Potential in the Appendix). Eq. 13 assumes that the fixed charge behaves like a uniformly charged plane in the center of the channel. This is, of course, not physically realistic. However, since the E field from the more physically realistic uniformly charged ring should have an E field and potential profile similar to that of the charged plane, Eq. 13 should provide a useful approximation to the fixed charge potential.

Diffuse Potential Φ

Since U and W are zero far away from the channel, the difference in the bulk solution value of Φ between the two sides of the membrane is equal to the applied membrane potential. All the complexity that results from the distribution of all the other ions in the system enters through Φ. The basic approach to solving the problem will be to assume a value for the flux and then solve for the value of $\Delta\Phi$ (or the applied voltage) necessary to produce this flux. The differential equation describing the spatial variation in Φ is again derived using the basic approximation ($E_\perp = 0$) and Gauss's law. If one draws a differential Gaussian surface in the channel with the two constant E surfaces separated by the distance dx (ρ = charge density and dv = differential volume element

$$\int_S E ds = (4\pi/\epsilon_w) \int \rho dv$$
$$-S(X)E(X) + S(X + dX)E(X + dX)dX$$
$$= (4\pi e/\epsilon_w)dX\Sigma z_i C_i S_i$$
$$-\frac{d}{dX}\left(S\frac{d\Phi}{dX}\right) = (4\pi e/\epsilon_w)\,\Sigma z_i C_i S_e^i. \qquad (14)$$

The S_e^i in Eq. 14 is the effective cross-sectional area of distribution of the ith ion at each position in the pore. It is significantly smaller than the geometrical pore radius and will be a function of, for example, the ion size and hydration. In contrast, S in Eq. 14 is the effective high dielectric region of the pore. It should be somewhat larger than the geometric pore radius to include the effect of the relatively high dielectric region that makes up the pore wall. The primary reason why the basic approximation greatly simplifies the problem is that it allows one to derive this simple differential equation for Φ. One could use more exact numerical solutions for U and W but it is difficult to find a numerical analogue to Eq. 14.

GENERAL SOLUTION FOR ION FLUX

Eq. 9 and 14 will be written in dimensionless variables (small case) with all distances normalized by the radius at the center of the pore (a) and the potentials normalized by $e/(a\epsilon_w)$ where e is the fundamental electronic charge (see Appendix for details). It will be assumed that the same solution is present on both sides of the membrane

$$j_i = -s_e^i g_i \Omega_i [c_i' + z_i \gamma c_i \psi_i'] \tag{15a}$$

$$\psi_i = u_i + w + \phi, \qquad u_i = z_i \phi_B/2 \tag{15b}$$

$$(s\phi')' = -\Sigma z_i \Omega_i c_i s_e^i. \tag{15c}$$

The prime indicates differentiation with respect to the dimensionless variable x. The potential functions ϕ, u_i, and w depend on the shape of the channel and the location and magnitude of the fixed charge. The approach used to solve this equation involves identifying one ion as the major ion and the rest as minor ions. Usually the major ion dominates the channel flux, although this is not essential. Variables written without the subscript or superscript i refer to the major ion. The details of the solution are described in the Appendix. The final result is the following third-order nonlinear differential equation for ϕ

$$\begin{aligned} s\phi''' = &-2s'\phi'' - \phi' s'' \\ &+ (s\phi'' + s'\phi')(s_e'/s_e - z\gamma\psi') \\ &+ z[j/g + \Sigma(z_i/z) j_i/g_i] \\ &+ z\gamma \Sigma z_i \Omega_i (z_i \psi_i'/z - \psi') c_i s_e^i \end{aligned} \tag{16a}$$

$$c_i(x) = [1 - (j_i/\Omega_i) I_i(x)] \exp(-\gamma z_i \psi_i) \tag{16b}$$

$$j_i = \Omega_i [1 - \exp(\gamma z_i \phi_0)]/I_i(\ell) \qquad \phi_0 = \phi(\ell) \tag{16c}$$

$$I_i(x) = \int_{-\ell}^{x} dx \exp(\gamma z_i \psi_i)/(g_i s_e^i). \tag{16d}$$

The choice of boundary conditions pose a special problem. An obvious option is to require that far away from the channel the concentration is equal to the bulk concentration and the gradients of C and Φ are equal to zero. However, since this condition implies that the flux is zero (Eq. 9), this condition can only be used for the equilibrium case. For the general case, it is necessary to assume that the bulk solutions are well-stirred up to some surfaces s_1 ($x = -\ell$) and s_2 ($x = +\ell$) on each side of the channel. The well-stirred condition implies that at these surfaces the ion concentrations are equal to those in the bulk solution and the solution is neutral. Thus, at these surfaces, one has the condition (see Eq. 14)

$$(s\phi')' = 0 \text{ on } s_1 \text{ and } s_2. \tag{17}$$

This provides two boundary conditions for the third-order differential equation. The third condition is provided by the fact that since only the relative value of the potential ϕ is important, ϕ can be arbitrarily set equal to zero on s_1. As the surfaces s_1 and s_2 are moved further away from the channel mouth, the solution should converge rapidly to some limiting value. In practice, the solution should be obtained at surfaces far enough from the channel mouth that the flux has reached its limiting value.

Since Eq. 16 is a nonlinear two point boundary value problem, its solution presents some problems. The procedure used was to choose some value for the flux j (the major ion). Then one make a guess for the value of ϕ' on s_1 and for j_i (the fluxes of the minor ions). The value of ϕ'' on s_1 is then determined from Eq. 17. The equation is then integrated across the channel to s_2 by a Runge-Kutta procedure to determine a new value for j_i and the value of ϕ' and ϕ'' at s_2. From the error when these values are substituted in Eq. 17, one makes a new guess for ϕ' at s_1 and repeats the procedure (using the new value of j_i) until the boundary condition at s_2 is satisfied. Then, the value of the applied membrane potential is equal to ϕ at s_2 (ϕ_0) and the flux of the minor ions is equal to the final (limiting) value of j_i.

The protocol that was followed was to first solve the equilibrium case (see below) for the value of ϕ' at s_1. This value of ϕ' was then used as the first guess for the nonequilibrium case with a very small flux (j). Then, j was increased in small steps and the previous values of ϕ' were used to extrapolate to the next guess. Proceeding in this way one could obtain the flux over a wide range of applied voltages (ϕ_0). At high concentrations and fluxes (applied voltages) the initial guess must be very close to the correct value or the integration across the channel blows up. This problem becomes severe as the potential energy wells get larger (i.e., valences of fixed charge and mobile ions of two or larger).

Solution for the Equilibrium Case

This case is of interest if one wishes to know the equilibrium ion concentration at the mouth of a charged channel or near a single fixed charge site on the surface of the membrane. It is also useful, as described above, for providing starting values for the integration in the general case. At equilibrium, the (dimensionless) concentration of the ith ion is described by

$$c_i = \exp(-\gamma z_i \psi_i) \qquad \psi_i = z_i \phi_B/2 + w + \phi. \tag{18}$$

Substituting these expressions into Eq. 15c yields a second-order nonlinear differential equation for ϕ. The associated boundary condition is again of the two point type with $\phi = 0$ on s_1 and s_2. If the channel is symmetrical, then ϕ' must equal zero in the center of the channel and the domain of integration can be reduced in half.

Solution for the Infinite Dilution Case

This case represents the limit in which the Nernst-Planck equation has classically been used. The only new contribution is that the applied potential profile is determined from the solution to Eq. 15c rather than, for example, assuming a constant gradient. From Eq. 15c, at infinite dilution ($c_i \rightarrow 0$)

$$(s\phi')' = -\Sigma z_i \Omega_i c_i s_\epsilon = 0. \tag{19}$$

This is an exact integral and the solution can be written in the form

$$\begin{aligned} \phi(x) &= BH(x) \\ B &= \phi_0/H(l) \\ H(x) &= \int_{-l}^{x} dx/s, \end{aligned} \tag{20}$$

where the integration goes from s_1 ($-\ell$) to s_2 ($+\ell$). For a pore of uniform cross section (constant s), the applied potential will have a linear profile (constant field) in the channel. Depending on the functional form of the channel cross-sectional area ($s[x]$), an analytical or numerical expression can be obtained for H. The value of the ion flux can then be determined immediately by substituting this expression for ϕ into the integrated solution of the Nernst-Planck equation

$$\begin{aligned} j_i &= \Omega_i[1 - \exp(\gamma z_i \phi_0)]/I_i(\ell) \\ I_i(\ell) &= \int_{-\ell}^{\ell} dx \exp(z_i \gamma \psi_i)/(g_i s_\epsilon), \end{aligned} \tag{21}$$

where ψ_i is defined by Eq. 15b and the integration required to determine I is performed numerically. The use of this simple solution depends on the validity of Eq. 19. This relation is rigorously satisfied in the infinite dilution case, but will also be satisfied if the solution is electrically neutral. Clearly, if a channel is ion selective, than it cannot be rigorously electrically neutral. However, this may be a useful approximation in some regions, e.g., in the bulk solutions approaching the channel, as was assumed by Lauger (5). To evaluate this assumption it will be necessary to compare it with the results of this more exact solution.

Solution for the Case Where the Flux of Some Ions are Zero

For most channels, one can assume that some ions are impermeant (e.g., anions in the gramicidin channel). This implies that in some region of the channel there is an additional infinite energy barrier for these ions. Although Eq. 16 could be solved by explicitly including this barrier, the following procedure is simpler. Let the kth ion be impermeant due to a channel region that completely excludes it. Then, the concentration of this ion on the left (c_k^-) or right (c_k^+) of this region is equal to

$$c_k^{\pm} = e^{-\gamma z_i[\psi_i(x) - \psi^{\pm}]} \tag{22}$$

where $\psi^{\pm}$ is equal to the potential in the left or right bulk solution and $c_k = 0$ in the excluding region. Eq. 16a can then be solved using this expression for c_k and $j_k = 0$.

Solution for Only the Entry and Exit Conditions

As discussed in the Introduction, one important application of this approach is to determine the access resistance of the channel mouth. In this case, one wants to apply Eq. 16 only to the bulk solution region without assuming that the channel itself can be described by this continuum approach. Although one cannot solve this problem in general because it requires detailed knowledge of the specific channel kinetics, the general approach that would be used and some special cases are discussed in the Appendix.

APPLICATION OF THEORY TO MODEL CHANNEL

The use of the theory will be illustrated by solving the equations for the channel with the geometry shown in Fig. 4. The channel is 32 Å long with a radius of 4 Å in the center and 8 Å at the ends. It will be assumed that all ions have a radius of 2 Å, except for one case when all have a radius of 1 Å. The surfaces s_1 and s_2 (up to which the bulk solution is assumed to be well stirred) are chosen as the hemispheres centered about the channel mouths. The solution will be presented for a fixed charge either at the center or end of the channel. Additional details are provided in the Appendix.

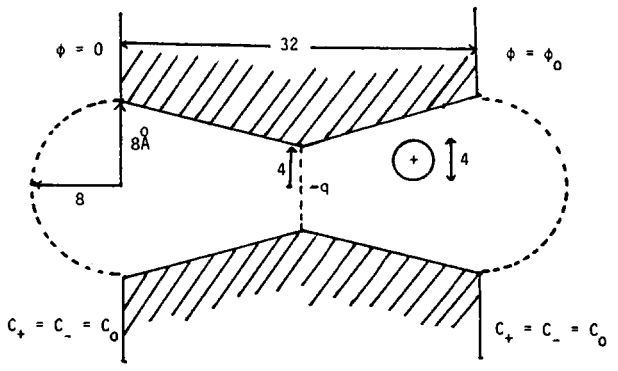

FIGURE 4 Diagram of the channel model. All dimensions are in angstroms. The bulk solution is assumed to be well-stirred up to the spherical region indicated by the dashed lines. The fixed charge is either at the center ($X = 0$) or left end ($X = -16$ Å) of the channel.

It is assumed that the effective area and diffusion coefficient are described by the continuum hydrodynamic equations (9)

$$S_e/S = (1 - \beta)^2, \qquad \beta = b/R \tag{23a}$$

$$D_e/D = 1 - 2.1044\beta + 2.08877\beta^3 - 0.947813\beta^5 - 1.372\beta^6 + 3.87\beta^8 - 4.19\beta^{10}, \tag{23b}$$

where b is the ion radius, R is the local pore radius, and D and D_e are the bulk and local (effective) pore diffusion coefficients. Eq. 23a for S_e assumes that the effective area is the area available for the center of the molecule. Eq. 23b for D_e is the effective diffusion coefficient in an infinitely long uniform cylindrical pore (this series solution is valid for $\beta \leq 0.5$). These two expressions obviously represent gross approximations, but they at least illustrate the main factors that would be needed for a more accurate solution. These corrections for the finite size of the ion have an important influence on the calculated fluxes. For an ion with a radius of 2 Å, β is 0.5 in the center of the channel (Fig. 4) where S_e is 1/4 S and D_e is ~1/6 D (the bulk diffusion coefficient). Since the contribution of the water of hydration probably depends on the pore wall structure and should vary with the pore diameter, the value of the ion radius will vary with position in the channel and is not well defined. For all ions in all the following cases it was assumed that the bulk diffusion coefficient (D) was 2×10^{-5} cm^2/s.

Monovalent Cation and Anion with Fixed Charge in Center of Membrane

Fig. 5 shows the profile for the Born image charging potential (U), the fixed charge potential (W), and for the sum of the two potentials for a channel with a fixed charge of valence −1 in the center of the channel. (For a fixed charge of valence −2, the fixed charge potential is doubled and the Born charging potential is unchanged.) For a channel of these dimensions (Fig. 4), the Born charging potential is small and the total potential is dominated by the fixed charge potential.

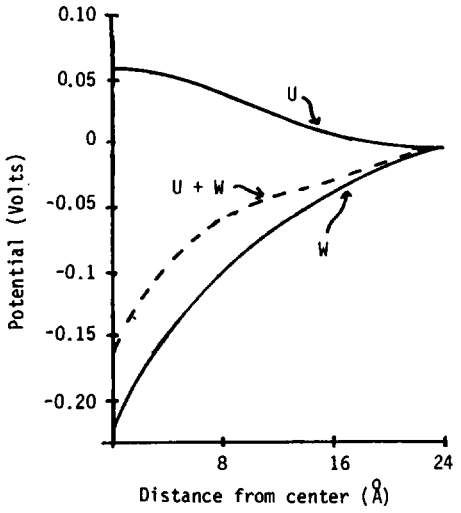

FIGURE 5 Born charging (U), fixed charge (W), and total ($U + W$) potential (volts) as a function of distance from the center of the symmetrical channel of Fig. 4. The fixed charge is at the center of the channel and has a valence of −1.

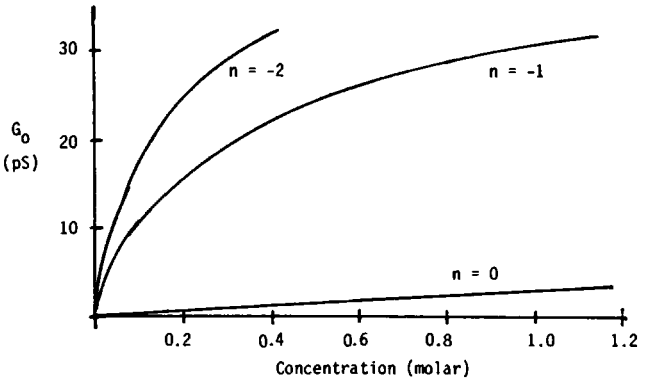

FIGURE 6 Single-channel conductance (picosiemens) of a monovalent cation in the limit of zero applied voltage for a fixed charge in the center of the channel with valence (n) of 0, −1, or −2 (ion radius = 2 Å).

Fig. 6 shows the cation conductance in the limit of zero applied voltage for a fixed charge of valence 0, −1, or −2. It can be seen that for the charged pore, the flux does tend to saturate as the concentration (ionic strength) is raised and the diffuse charge screens the fixed membrane charge. The conductance never completely levels off (as would be expected for simple binding to a single fixed site) since even when the fixed change is completely screened the conductance should still increase with concentration in the same way as in the uncharged ($z = 0$) channel. The charged channel shows a strong discrimination between cations and anions. In the low concentration limit, the anion conductance is ~10^{-5} that of the cation for a fixed charge of −1. The conductance ratio decreases to 5×10^{-3} as the concentration is increased to 1.14 M and the fixed charge becomes screened by the counter ions. The discrim-

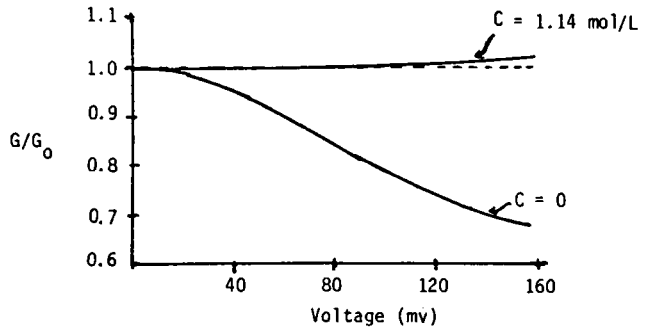

FIGURE 7 Conductance at indicated voltage relative to conductance in the limit of zero applied voltage (G/G_o) at low ($C = 0$) and high ($C = 1.14$ M) concentrations. (Fixed charge [valence = −1] in center of channel, ion radius = 2 Å).

ination is, of course, larger for a fixed charge of -2, with a conductance ratio of $\sim 10^{-9}$ at low concentrations and 10^{-4} at a concentration of 0.39 M. In the uncharged channel ($n = 0$) the flux of the cation and anion are equal and opposite.

The current voltage (I-V) characteristics of this channel is shown in Fig. 7 for the infinite dilution case ($C = 0$, Eq. 21) and for a high concentration (1.14 M). The I-V curve is quite sublinear at the low concentrations and becomes nearly linear (0–160 mV) at the high concentration.

In this continuum model, the ion is completely characterized by two parameters: the charge and radius. Differences in conductance or apparent saturation constants for different monovalent cations can only result from differences in their effective radii. Fig. 8 compares the conductance vs. concentration curves for cations with radii of 1 and 2 Å. It is assumed in these calculations that both ions have the same bulk diffusion coefficient so that any difference in the flux results from different discrimination by the channel. The conductance of the 1 Å ion is about twice that of the 2 Å ion over the entire concentration range.

Monovalent Cation and Anion with Charge at the End of the Channel

Fig. 9 shows the profiles of the potential (W) for a fixed charge of valence $= -1$ at the left end ($x = -16$ Å) of the channel along with the Born charging (U) and the total potential. The well depth of the fixed charge potential is smaller when the charge is at the channel end (compare Figs. 5 and 9) because the field lines can spread directly into the bulk solution and are not constrained to the relatively narrow channel. Fig. 10 shows the cation and anion conductnce in the limit of zero applied voltage for a fixed charge of valence (n) $= 0$ and -1. The cation conductance is ~ 10 times smaller than when the charge is in the center of the channel and the discrimination against anions is much less, with an anion to cation conductance

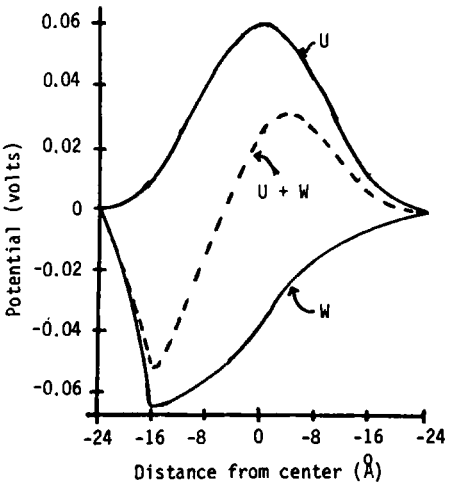

FIGURE 9 Born charging (U), fixed charge (W), and total ($U + W$) potential as a function of the position of the monovalent cation. The fixed charge has a valence of -1 and is located at the left end ($X = -16$ Å) of the channel. A positive applied potential produces a cation flux from left to right.

ratio varying from 0.065 in the low concentration limit to 0.47 at a concentration of 0.69 M when the fixed charge is partially screened. The reduced effect of the fixed charge when it is at the end of the channel results not only from the smaller magnitude of the potential but also because of its specific location. The peak of the Born charging potential barrier to ion flux is at the center of the membrane. The fixed charge has its maximum influence on this barrier when it is also in the center of the membrane, lowering the barrier for cations and raising the barrier for anions. When the fixed charge is at the channel end, its influence on this central barrier is reduced (compared Figs. 5 and 9).

Fig. 11 shows the voltage dependence of the cation conductance at low and high concentration (0.69 M). As is expected for this asymmetric channel, the conductance is also asymmetrical. The asymmetry is greatly reduced at high concentrations when the fixed charge (the cause of the asymmetry) is screened by counter ions.

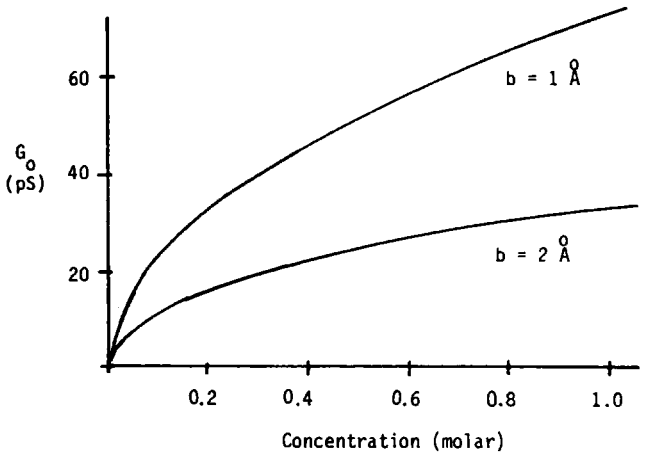

FIGURE 8 Effect of ion radius (b) on conductance ($n = -1$, see Fig. 6).

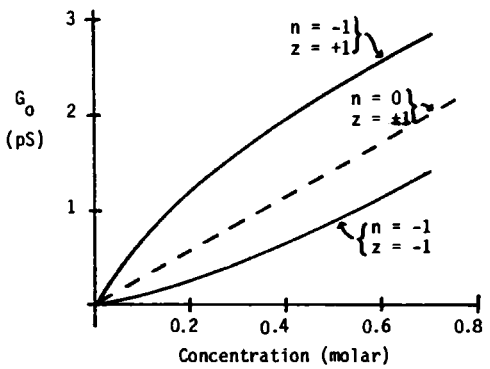

FIGURE 10 Zero voltage limiting conductance as a function of concentration for a fixed charge with valence (n) of either -1 or 0 located at the left end of the channel. The conductance is shown for ions with valence (z) of -1 and $+1$.

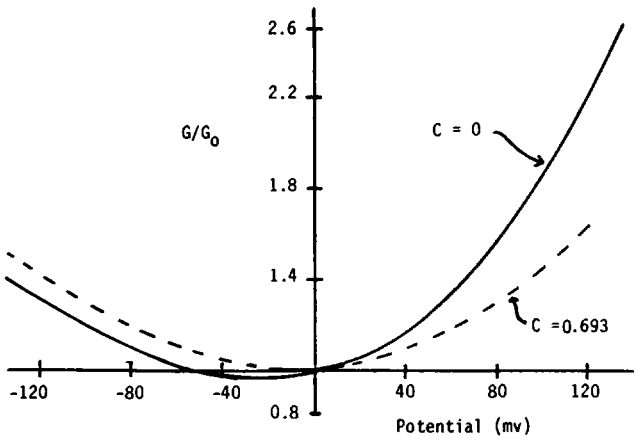

FIGURE 11 Voltage dependence of conductance of monovalent cation in a channel with a fixed charge of -1 at the left end for low (C = 0) and high (C = 0.693) concentrations.

Divalent Cation with Charge in the Center of the Channel

It is usually assumed that the channel conductance of a divalent ion should be less than that of monovalent because the repulsive Born charging potential (see Eq. 11) is proportional to the valence while the other (attractive) potentials are independent of valence. However, for this channel model (Fig. 4) the Born charging potential is so small that the total potential (Fig. 12) is still attractive (negative) for divalent cations. Since the energy barrier is equal to the potential energy times the valence of the ion, this channel is more attractive for divalent than monovalent cations and, in the low concentration limit, the divalent conductance (Fig. 13) is ~2.6 times greater than the monovalent conductance (Fig. 6). As can also be seen in

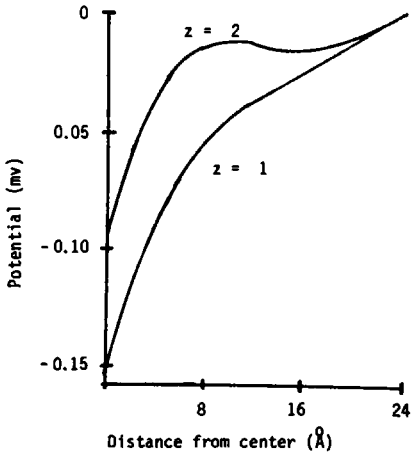

FIGURE 12 Comparison of total potential of a monovalent (z = 1) and divalent (z = 2) cation in a channel with a fixed charge of -1 in the center. The Born charging and fixed charge potential for the monovalent cation are shown in Fig. 5. For the divalent cation, the fixed charge potential is equal to and the Born charging potential is twice that of the monovalent cation.

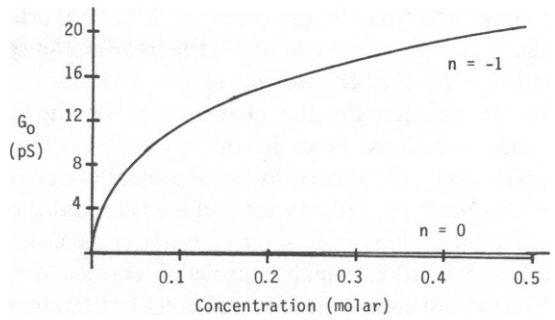

FIGURE 13 Zero voltage limiting conductance of a divalent cation in a channel with a fixed charge (n) of either 0 or -1 in the center.

Fig. 13, the divalent conductance of the channel shows some saturation at very low concentrations. For example, at 1 mM the conductance normalized for concentration (G_o/c) is reduced by ~30% from its zero concentration limiting value. As the concentration is raised, the fixed charge is further screened and at high concentrations the divalent conductance is less than the monovalent conductance. In the absence of a fixed charge (n = 0) the Born image potential barrier dominates and the conductance is only $\sim 10^{-3}$ that with a fixed charge of $n = -1$ (Fig. 13).

The conductance was also determined for one case where both monovalent and divalent cations (and monovalent anions) were present (all with a radius of 2 Å). Fig. 14 shows the low voltage limiting conductance for the case where the monovalent cation concentration is equal to five times the divalent concentration. At very low concentrations (<1 mM), the fixed charge is not screened so that the conductance of the two cations are independent and similar to that when they are present by themselves (Figs. 6 and 13). As the concentration is raised, the divalent conductance rapidly saturates and even decreases slightly at high concentrations.

DISCUSSION

The use of the basic approximation that the ratio of the dielectric constant of the water to the lipid is infinite allows one to derive relatively simple analytic expressions for the

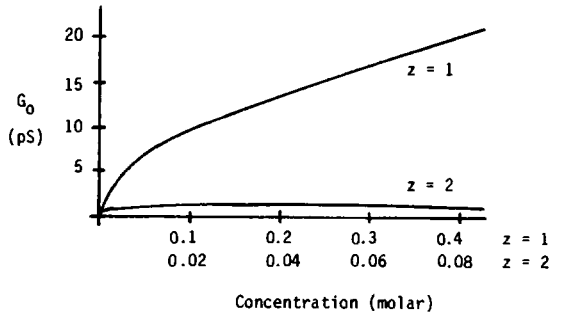

FIGURE 14 Zero voltage limiting conductance of the monovalent (z = 1) and divalent (z = 2) cation in a channel with a fixed charge of -1 in the center. The concentration of the divalent is always one-fifth that of the monovalent.

Born image and fixed charge potential. More importantly, it leads to a differential equation (Eq. 14) for the spatial dependence of the applied potential. This leads to a continuum solution for the channel flux or the access resistance, which is exact in the same sense that the Debye-Huckel (10) theory for strong electrolytes or the Gouy-Chapman (11) theory for surface potential is exact. The main limitation of this solution is not in the use of this basic approximation, which is probably correct to within 10–20% in most cases, but in the inherent limitation of this type of continuum approach. For example, consider a channel that has one fixed negative charge in its center. The presence of just one cation in the channel to the left of this charge will completely screen the charge from another cation entering the left end. Thus, the screening is nearly all or none, with the probability that the charge is screened increasing with the bulk cation concentration. This continuum approach essentially assumes that one can replace the probability that the charge is screened at any one time by the time average of the screening and it completely neglects the fact that, as an ion passes through the channel, the potentials at different times will be correlated. A specific example of the type of error introduced by the continuum assumption is provided by the numerical simulation of Cooper et al. (12). The validity of this assumption is difficult to evaluate in the absence of an exact solution to compare it with. It is probably quite good for equilibrium situations. For example, the calculation of the potential at the mouth of the pore represents only a slight variation of the Gouy-Chapman solution for the surface potential and it should have the same range of validity. For nonequilibrium cases, the approximation should be better when it is limited to the bulk solution, such as in the calculation of the access resistance where this approach is clearly the best available and represents a significant improvement over previous solutions (5, 6).

Another source of error in this continuum solution is in the choice of the functions to represent the effective areas (S_e) and diffusion coefficient (D_e) in the channel. The classical continuum solution used here for D_e (Eq. 23b) is not exact for tapering channels and neglects the influence of other ions in the channel. If the channel is narrow enough that single-file effects become important (13), then the use of the continuum expression for D_e is qualitatively incorrect. Most important is the uncertainty introduced in defining an effective ion radius. Since the radius depends on the number and strength of the waters of hydration, it is not a real physical parameter. For the channel model used here, the influence of the finite ion size on the channel conductance is quite large. For example, the conductance approximately doubled when the ion radius decreased from 2 to 1 Å (with no change in bulk diffusion coefficient).

The application of this approach to the complete channel flux, as was illustrated in this paper for the channel of Fig. 4, provides a new alternative approach to modeling ion channel kinetics that may, for some channels, present clear advantages over the other two commonly used approaches: the classical Nernst-Planck solution and the reaction-rate method. This new approach seems particularly well suited for the type of channel modeled here (Fig. 4), where the selectivity is determined primarily by simple steric and long-range electrostatic effects. The channel is large enough that the ion kinetics should be close to a continuum diffusive mechanism without any identifiable binding sites or energy barriers. This makes the reaction-rate model a particularly poor physical representation of this type of channel. The problem with the classical Nernst-Planck approach is that it only applies to the situation where there is no ion-ion interaction. Although it is possible to modify the equations to explicitly include ion-ion effects (13), this leads to a very complicated numerical problem. In addition, the channel is so large (especially when the bulk solutions at the channel mouth are included), that it may be necessary to allow for the interaction of a large number of ions and this would pose formidable problems for these two classical approaches.

Despite the uncertainties and inherent limitations of this continuum approach, it has the major advantage that is relatively simple and incorporates most of the relevant features that one would expect from an accurate solution. The channel is completely characterized by its shape and the location of the fixed charges; a level of detail that is about at the current limit of resolution of biological membrane channels.

The acetylcholine receptor channel is an obvious candidate for the application of this approach (15). It is cation selective and the permeability ratios of the monovalent inorganic (16) and organic (12) cations can be described fairly accurately by the simple continuum theory. The channel also has a significant permeability for the divalent inorganic cations (about one-fifth that of the monovalent cations) and shows very little discrimination between the different divalents (17). The limiting radius of the model used here (4 Å, Fig. 4) was chosen to be similar to the radius of the largest ions that could pass through the acetylcholine channels so the qualitative features of this model could be compared with the experimental results on the acetylcholine channel. There is a major discrepancy between the model and experimental results for the concentration dependence of the conductance. The single channel conductance saturates with kinetics that are similar to what would be predicted for a single simple binding site (18), while the model conductance, although showing some saturation, does not level off at a maximum value. This discrepancy illustrates the most important limitation of this continuum model where the ion-ion interaction results only from the diffuse screening of the fixed charge. It lacks the strong interaction that would result, for example, from one ion blocking the channel at a restricted region by a single file mechanism. However, there is enough qualitative agreement between the model and

experimental results (single-channel conductance, I-V relations, saturating concentrations, cation vs. anion and divalent vs. monovalent selectivity) to at least suggest that the basic features of the model may be correct.

The essential feature of this model is that the selectivity results from simple steric and long-range electrostatic effects and that there are no specific binding sites. The classical qualitative test for such electrostatic effects is to vary the ionic strength by adding different impermeable electrolytes and show that any inhibition of the flux is a function only of the ionic strength and does not depend on the specific cation. However, this test will not work for the channel model of Fig. 4 because the inhibition produced by the screening of the fixed charge by an impermeant monovalent cation will depend on the depth the ion can reach in the channel and, therefore, on the effective radius of the cation. This prediction is born out for the acetylcholine channel where most cations either conduct or block (or both) to varying degrees and no such nonspecific cation has been found.

As discussed above, the basic limitation of this model is its inability to simulate the strong ion-ion interaction that should occur at some locations in most ion channels. Probably the most direct way to introduce this interaction is by using a hybrid of this continuum approach with the reaction-rate model. Thus, this continuum solution would be used for the regions of the channel where the ion-ion interaction was weak and could be modeled by the diffuse screening, whereas the reaction-rate model would be used for the limited region where strong ion-ion interactions would be expected. The two solutions could be combined as described in the Appendix for the determination of the access limitation at the channel mouth.

APPENDIX

Derivation of Eq. 16

One ion species is chosen as the major ion and is written without a subscript. Solving Eq. 15c for c

$$c = B - \sum_i (z_i/z)\,(s_e^i/s_e)\,(\Omega_i/\Omega)\,c_i \quad B = -(s\phi')'/z\Omega s_e \qquad \text{(A1)}$$

where the summation is over the minor ions. Differentiating Eq. A1

$$c' = B' - \sum_i (z_i/z)\,(\Omega_i/\Omega)\,(s_e^i/s_e)\,c_i'. \qquad \text{(A2)}$$

Solving Eq. 15a for c_i'

$$c_i' = -j_i/(g_i\Omega_i s_e) - z_i\,\gamma\,c_i\,\psi_i' \qquad \text{(A3)}$$

Eq. 15a can be written as

$$j = -(g\Omega s_e)\,(c' + z\gamma c\psi'). \qquad \text{(A4)}$$

Finally, substituting Eq. A3 for c_i' into Eq. A2, Eq. A1 for c and Eq. A2 for c' into Eq. A4, and solving for ϕ''', yields Eq. 16a of the text. Eqs. 16b–d are the conventional integrated form of the Nernst-Planck equation.

Details of Numerical Solution

Eq. 16 is solved subject to the two boundary conditions of Eq. 17 and the third condition that $\phi = 0$ on the left boundary ($x = -\ell$). An iteration procedure is used. A very small value of j is chosen (so that the system is close to equilibrium) and the value of ϕ' at $-\ell$ determined from the equilibrium solution (Eq. 18) is chosen as a first guess. In addition, during each iteration, the values of j_i must be chosen. For the first iteration j_i is chosen to be zero. The values of $c_i(x)$ needed in Eq. 16a are determined from Eq. 16b. Eq. 16a is then integrated to $x = +\ell$ by a Runge-Kutta procedure. At this boundary ϕ' and ϕ'' are determined and the deviation from the boundary condition (Eq. 17) is determined. The procedure is then repeated, picking a new ϕ' at $x = -\ell$ by extrapolating the proceeding values to minimize the deviation in the boundary condition at $x = \ell$, and using the proceeding values of j_i to extrapolate to the next j_i. After finding the solution for this initial choice of j, j is incremented and the previous values of ϕ' at $x = -\ell$ and j_i are used to extrapolate for the initial guess of the new values. The pore model used here (Fig. 4) has a discontinuity in s' and therefore an infinity in s''. The integration across these infinities is performed analytically. The general numerical solution was checked by comparing it with the special solutions for the two limiting cases of infinite dilution ($C \to 0$; Eq. 21) and equilibrium ($J \to 0$; Eq. 18).

Access Resistance at Pore Mouth

This is the case referred to in the Introduction where one wants to apply the exact continuum solution developed in this paper to the bulk solutions on each side of a channel whose kinetics are assumed to be previously determined (e.g., in terms of a reaction-rate mode). The particular solution for the channel proper should provide a description of the flux in terms of the permeable ion concentration and the applied potential difference in the bulk solutions just outside the channel. The most common application would be for the case where there is only one permeable cation along with impermeable anions and possibly other inert (i.e., impermeable) electrolytes. The general solution for this case is described here.

The bulk solution regions of the system are again described by the same differential equations (Eq. 16) and boundary conditions (Eq. 17). As before, a value for the ion flux is assumed and a first guess is made for the value of ϕ' at the left boundary. The concentration of the impermeant ions (subscript i) is described by Eq. 18. Eq. 16 is then integrated up to the pore mouth where the value of ϕ, ϕ', and ϕ'' are determined. The concentration of the permeant ion (no subscript) at the pore mouth is then determined from Eq. A1. Since ϕ and $s\phi'$ must be continuous across the boundary between the pore and bulk solution (see Eq. 15c), the value of ϕ and $s\phi'$ at left end of the pore is known. It will be assumed, as is normally done in the reaction-rate approach, that the applied potential varies linearly in the pore (or, somewhat more generally, that $s\phi'$ is constant in the pore). The value of the applied potential drop across the pore can then be determined from $s\phi'$ at the left end and the length (and cross-sectional area, s) of the pore. Then, the flux equation for the pore can be solved for the concentration in the bulk solution at the right end of the pore from the known ion flux, potential difference, and concentration at the left end. This uniquely determines the initial conditions for the integration over the bulk solution at the right end of the pore. The values of ϕ and $s\phi'$ are known at the right since they are continuous across the pore end and ϕ'' can be determined from ϕ' and the concentration using Eq. A1. Then, the integral across the right bulk solution is carried out and the iteration procedure is repeated as discussed above until the boundary condition at the right boundary is satisfied. The importance of the bulk solution access resistance can then be determined by comparing the flux with the predicted flux if the bulk solutions were not limiting (for the same concentration and potential difference).

For the limiting case where the conductance of the pore is infinite relative to the bulk solutions, the access resistance can be determined uniquely without knowing any details about the pore kinetics. The only place in the above general approach where the pore kinetics were used was

to solve the flux equation for the concentration at the right end of the pore. For this limiting case, the pore ends must be in equilibrium and the concentration can be determined from the Boltzmann relation and the known potential drop and concentration at the left end.

Analytical Expressions for Born Image and Fixed Charge Potential

The derivation of the Born image potential in the text was for the case where the ion was in the center of a symmetrical channel. The derivation will be given here for the ion at an arbitrary position in the channel proper ($-\delta < y < \delta$). Close to center of the ion the E field should be identical to that in a homogeneous aqueous solution. It will be assumed that within a distance $r(y)$ (the radius of the channel at the position $[y]$ of the ion) the field is equal to the homogeneous field

$$\begin{aligned} e^{\pm}(x) &= \pm e_H(x - y) \qquad |x - y| < r(y) \\ e_H(x) &= n/x^2, \end{aligned} \tag{A5}$$

where n is the ion valence and the + and − refer to the field on the right and left of the ion. For values of x greater than one ion radius and within the pore region of Fig. 4 ($-\ell < x < \ell$, including the aqueous region at the mouth), the E field can be determined by using two Gaussian boxes with one end of each box through the center of the ion and the other end either to the left (−) or right (+) of the ion. Defining the field and surface area at the center of the ion equal to e_o and s_o, the value of $e^{\pm}$ is obtained from the application of Gauss's law to each box

$$\begin{aligned} e^{\pm}(x) &= (e_0 s_0 \pm 2\pi n)/s(x); \\ &\qquad |x - y| > r(y) \text{ and } |x| < \ell \\ &= 2\pi n(\alpha \pm 1)/s(x), \end{aligned} \tag{A6}$$

where e_o has been defined in terms of another unknown ($\alpha = e_o s_o/2\pi n$). The area of the constant E surface $s(x)$ is defined by Eq. 6 with the local radius used in place of a. For the pore of Fig. 4, the local radius (r) is equal to $1 + |x|/\delta$ and the radius at the end of the pore (r_o) is equal to two. For regions outside the pore region the E field is equal to the homogeneous field for a radius centered about the mouth of the channel

$$e^{\pm}(x) = (\alpha \pm 1)\, e_H(|x| - \delta) \qquad |x| > \ell. \tag{A7}$$

Then, the total potential in going from the bulk solutions on either the left (ϕ_T^-) or right (ϕ_T^+) side is equal to

$$\begin{aligned} \phi_T^{\pm} = -\int_{\pm\infty}^{y} e^{\pm}\,dx &= -(\alpha \pm 1)\int_{\pm\infty}^{\pm r_0} e_H\,dx \\ &\quad - \int_{\pm(r_0\pm\delta)}^{y\pm r(y)} e^{\pm}\,dx \mp \int_{\pm r(y)}^{0} e_H\,dx. \end{aligned} \tag{A8}$$

The potential at the ion in the bulk solution (homogeneous) is equal to

$$\phi_H = \int_{-\infty}^{-r_0} e_H\,dx + \int_{-r_0}^{y-r(y)} e_H\,dx + \int_{r(y)}^{0} e_H\,dx. \tag{A9}$$

The Born image potential is the difference between the total and the homogeneous potential (using Eq. A5 for e_H):

$$\begin{aligned} \phi_B^{\pm} &= -\alpha n \int_{\pm\alpha}^{\pm r_0} dx/x^2 + \int_{-r_0}^{-r(y)} dx/x^2 \\ &\quad - \int_{\pm(r_0+\delta)}^{y\pm r(y)} e^{\pm}\,dx \\ &= \pm\, \alpha n/r_0 + n[1/r_0 - 1/r(y)] \\ &\quad - \int_{\pm(r_0+\delta)}^{y\pm r(y)} e^{\pm}\,dx, \end{aligned} \tag{A10}$$

where $e^{\pm}$ is given by Eq. A6. The value of the parameter α is determined from the condition that the value of ϕ_B must be the same when approached from either bulk solution ($\phi_B^+ = \phi_B^-$). The solution for ϕ_B then involves several integrals over the $s(x)$, which can be written in analytical form. Analytical expressions for the first and second derivative of ϕ_B (needed in Eq. 16) can also be determined. Since this approach cannot be simply extended to ions located outside the channel, ($|y| > \delta$) the value of ϕ_B in these regions was defined by arbitrarily extrapolating ϕ_B to zero at $|z| = \delta + r_o$.

$$\phi_B = \phi_B(\delta)(\delta + r_0 - y)^2/r_0^2 \qquad \delta < |y| < \delta + r_0. \tag{A11}$$

Since ϕ_B is relatively small in this region, any error introduced by this assumption is negligible.

The derivation for the potential for a fixed charge at an arbitrary position (y) in the pore follows a similar procedure. The E field to the left (e^-) or right (e^+) of the fixed charge is again given by Eq. A6 where n is now the valence of the fixed charge. The potential at the charge ($u_\pm[y]$) can be obtained by integrating from the bulk solution on either the left or right side

$$u_{\pm}(y) = -\int_{\pm(\delta+r_0)}^{y} e^{\pm}\,dx. \tag{A12}$$

The integration starts from the surface of the bulk solution region at the pore mouth [$\pm(\delta + r_o) = \pm\ell$] because, by definition, the solution is well-stirred up to this point and therefore the fixed charge potential must be zero up to this position. The value of α is determined from the equality $u_+(y) = u_-(y)$. The fixed charge potential is then given by Eq. A12 for x to the left (u_-) or right (u_+) of the fixed charge.

This work was supported in part by a grant from the National Institutes of Health (GM 25938).

Received for publication 6 November 1984 and in final form 13 February 1985.

REFERENCES

1. Jordan, P. C. 1984. The total electrostatic potential in a gramicidin channel. *J. Membr. Biol.* 78:91–102.
2. Monoi, H. 1983. Ionic interactions and anion binding in the gramicidin channel. An electrostatic calculation. *J. Theor. Biol.* 102:69–99.
3. Levitt, D. G. 1978. Electrostatic calculations for an ion channel. I. Energy and potential profiles and interaction between ions. *Biophys. J.* 22:209–219.
4. Bell, J. E., and C. Miller. 1984. Effects of phospholipid surface charge on ion conduction in the K^+ channel of sarcoplasmic reticulum. *Biophys. J.* 45:279–287.
5. Lauger, P. 1976. Diffusion-limited ion flow through pores. *Biochim. Biophys. Acta.* 455:493–509.
6. Andersen, O. S. 1983. Ion movement through gramicidin A channels. Interfacial polarization effects on single-channel current measurements. *Biophys. J.* 41:135–146.
7. Halliday, D., and R. Resnick. 1976. Physics. Part 2. John Wiley & Sons, Inc., New York. 606–614.
8. Jordan, P. C. 1982. Electrostatic modeling of ion pores. Energy barriers and electric field profiles. *Biophys. J.* 39:157–164.
9. Bean, C. P. 1972. The physics of porous membranes — neutral pores. *In* Membranes. G. Eisemann, editor. Marcel Dekker, Inc., New York. 1:1–54.
10. McQuarrie, D. M. 1976. Statistical Mechanics. Harper and Row, New York.
11. McLaughlin, S. 1977. Electrostatic potentials at membrane-solutions interfaces. *Curr. Top. Membr. Transp.* 9:71–144.

12. Cooper, K., E. Jakobsson, and P. Wolynes. 1983. Brownian dynamic analysis of ion movement in membranes. *Biophys. J.* 41(2, Pt. 2):47*a*. (Abstr.)
13. Levitt, D. G. 1984. Kinetics of movement in narrow channels. *Curr. Top. Membr. Transp.* 21:181–197.
14. Levitt, D. G. 1982. Comparison of Nernst-Planck and reaction-rate models for multiply occupied channels. *Biophys. J.* 37:575–587.
15. Barry, P. H., and P. W. Gage. 1984. Ionic selectivity of channels at the end plate. *Curr. Top. Membr. Transp.* 21:1–51.
16. Adams, D. J., T. M. Dwyer, and B. Hille. 1980. The permeability of endplate channels to monovalent and divalent metal cations. *J. Gen. Physiol.* 75:493–510.
17. Dwyer, T. M., D. J. Adams, and B. Hille. 1980. The permeability of the endplate channel to organic cations in frog muscle. *J. Gen. Physiol.* 75:469–492.
18. Dani, J. A., and G. Eisenman. 1984. Acetylcholine-activated channel current-voltage relations in symmetrical Na^+ solutions. *Biophys. J.* 45:10–12.